Fractured reservoir characterization using borehole electrical images and dipole sonic data: a Bolivian case.

Carlos A. Gonçalves[1], Marco Sanguinetti[1], J. C. Glorioso[2]

[1]Schlumberger Geoquest,

[2]Maxus Bolivia Inc

Abstract

Major gas trends have developed in South Bolivian reservoirs. The reservoir rocks are often very hard formations, extremely fractured, and with virtually no primary porosity. Through the use of wellbore imaging and other logging techniques, stress-induced compressive failure and tensile failure of the wellbore wall can be detected, and shear failure (i.e., slip along preexisting shear faults) can be identified.

We present a combined technique that exploit wellbore electrical image and dipole sonic data which enable a complete fracture characterization. In the absence of core data, FMS* Formation MicroScanner, FMI* Fullbore Formation MicroImager and DSI* Dipole Sonic Imager wireline logs provided valuable geologic information.

The high-resolution geologic interpretations of the FMS and FMI data were able to routinely identify fractures in the wireline resistivity images. Image features are oriented in space, and quantitatively characterized, with their density, aperture and porosity estimated.

INTRODUCTION

The estimation of hydrocarbon reserves is a complex topic in the presence of naturally fractured reservoirs. Most fractured reservoirs are characterized by low matrix porosities (less than 5%) and low matrix permeability (< 1md). For those reservoir characteristics, it is quite hard to get a reliable value of the original hydrocarbon in place. Thus, the importance in fully characterizing natural fractures, not only qualitatively, but also quantitatively.

But how big is fracture porosity? The answer is that it can be as large as 100%, depending on the scale you are analyzing them. At a reservoir scale, the average value is less than 1% (Aguillera, 1995), but the literature has shown cases where fracture porosity is as great as 4%. Although the porosity value is generally very low, the storage of hydrocarbons in fractured systems can be very large, due to the generally high interconectivity of a fractured zone.

Natural fractures generally exhibit certain characteristics. They are usually normal to the structural dips of the formations, but it does not exclude the possibility of horizontal fractures or fractures parallel to the structural dips to be present. The latter are less frequent and generally less extent than the subvertical ones, but can play an important role in the reservoir characterization.

Fracture detection and characterization using wireline log data have been performed for a long time, but the results achieved were not always satisfactory. Historically, the oldest fracture indicators are the sonic measurement and the dipmeter measurements. The use of new techniques such as the downhole electrical images (both FMS and FMI) and the dipole sonic imager (DSI) have increased the ability to characterize fractures *in situ* through the high resolution images produced by the FMS and FMI and the use of a combination of compressional, shear and stoneley waves from the DSI.

BOREHOLE ELECTICAL IMAGES AND THE DIPOLE SONIC IMAGER

DSI Dipole Shear Sonic Imager

The DSI tool combines dipole and monopole technologies for enhanced measurements of shear, compressional and stoneley waveforms, both in hard and soft formations. Each of the eight receiver stations, spaced 6 in. apart vertically, consists of four hydrophone elements mounted circumferentially 90 degrees apart, making a total of 32 hydrophones. Each sonic waveform can be defined by up to 15,000 samples of variable length.

Processing of the DSI data provides the slowness of the different waveform components, using either slowness-time-coherence or downhole first motion-detection techniques. These slownesses have applications in geophysical, petrophysical and mechanical property evaluations. The slowness-time-coherence (STC) and the variable density log (VDL) presentations can be used to show the effect of fractures detected by the wave train. A sharp increase in the amplitude of the compressional and the shear first arrivals can be easily identified in front of naturally fractured zones.

* Mark of Schlumberger

FMS/FMI Borehole electrical images

In conductive muds, the FMS and the FMI tools provide electrical images almost totally insensitive to borehole conditions and offer quantitative information, particularly for fracture analysis. They combine high-resolution measurements with almost fullbore coverage in standard diameter boreholes. The processed borehole images allows for the interpretation of the formation features such as structural dips, naturally open, healed and mechanically induced fractures, and other internal bedding features such as cross-bedding (Schlumberger, 1989).

Some of the more common applications of the electrical borehole images are: structural analysis, characterization of sedimentary bodies, enhanced textural analysis and complete fracture network evaluation. In both static and dynamic normalyzed images, open fractures appear as dark (conductive) features in the images, while healed (or mineral filled) fractures appear as light (resistive) features, both generally perpendicular to the structural dips. There are cases where producing open fractures can appear as light (resistive) patterns in the images. This is the case where those fractures are impregnated with hydrocarbon.

FRACTURE DENSITY, APERTURE AND POROSITY

In order to obtain an estimate of the open fracture porosity, a certain procedure must be followed. This procedure includes the computation of the fracture density and the fracture aperture, or the width of the fracture seen on the images.

Fracture density is determined by computing the number of open fractures per meter of logged interval. Thus, a control of the densest fractured intervals can be obtained.

The computation of fracture aperture (Luthi and Souhaite, 1990) can be achieved through the equation:

$$W = c * A * Rm^{b} * Rxo^{(1-b)}$$

where,

W is the fracture aperture;
b and **c** are tool constants;
A is the applied current divided by the voltage and integrated over an interval normal to the fracture direction;
Rm is the mud resistivity;
Rxo is the flushed zone resistivity.

As we can see, for high Rm values, fracture aperture should increase, while low Rm values would decrease fracture aperture. In the other hand, high Rxo values would decrease fracture aperture, while low Rxo values would lead to high fracture apertures. Therefore, the quality control of these two parameters are of crucial importance when computing fracture apertures. There are several ways for estimating fracture porosity (Nelson, 1995; Aguillera, 1995). Although each of them differ from the others in one or other aspect, most of them use the same parameters such as the mean aperture and the average spacement between fractures, and even important, they are all scale-dependant (Nelson, 1995). While primary (matrix) porosity depend on grain size and the arrangement of the grains, fracture porosity depends on the spacement between fractures, or the inverse of their density.

RESULTS FROM WELL XX

The main goal in running the Formation Microscanner and the Formation MicroImager tools in well XX was to determine the structural characteristics of the sediments, mainly giving by tectonic fracturing. The total logged interval (X396-X820 meters) is divided in two runs: the upper part (X396-X530 meters) was run with a combination of FMI and DSI, while the lower section (X530-X820 meters) was run with a FMI/DSI combination. The whole interval consists of massive sandstones, massive/laminated shales and laminated sandstones/siltstones.

The focus of the interpretation was mainly to characterize the tectonic fracturing, through the determination of fracture type, density, aperture and porosity (the latter three for open fractures only). During interpretation, different sets of geological features such as structural bedding, erosive surfaces, laminations, cross-bedding, induced fractures, etc., were also identified, but they will not be fully described because of the objectives of this work.

Open fractures were observed in both upper and lower sections of the well. One set strikes ESE-WNW, dipping between 55^{o} to 80^{o} to SSW (180^{o} to 220^{o}); the second set strikes ENE-WSW and dips 50^{o} to 70^{o} to SSE (140^{o} to 180^{o}); a third set, also striking ESE-WNW, shows dips between 10^{o} and 35^{o} to NNE; a fourth set striking ENE-WSW with dips between 65^{o} and 90^{o} to NNW was also detected (Figure 1). The strike of the fractures is perpendicular to the direction of minimum horizontal stress in the region and the axis of the main structures. In both static and dynamic FMS and FMI images, open fractures are generally identified by continuous and non-continuous sinusoids, electrically conductive events that have been filled by mud after drilling.

In the VDL display of the waveform trend, “chevron” patterns also indicate the presence of open fractures. These patterns are generated by an increase in wave amplitudes in front of these zones. Other way to identify open fractures is through the STC display, where these features usually destroy the shear wave signal (Figure 2). Another possibility is through the computation of the attenuation of the stoneley wave energy (Figure 2). WAVENE* processing in

GeoFrame allows for computing the energy of compressional, shear and stoneley waves and differential of the waveform energy. Stoneley are typically used to identify the location of fractures because the existence of a fracture absorbs the energy of the waveforms. In the example of Figure 2, it is possible to see the correlation between dense fractured zones, STC bad shear signal and the high energy attenuation.

Fracture aperture in well XX ranges mainly from 0.001 to 0.1 mm. In the upper section (FMI logged), it is possible to distinguish two main groups of fracture apertures. The first one, related to the open fractures striking ESE-WNW, has higher values, ranging from 0.008 to 0.1 mm, with an average value of 0.04 mm. The second group is related to the open fractures striking ENE-WSW, which shows apertures from 0.006 to 0.03 mm and average value of 0.01 mm. In the lower section (FMS logged), apertures are narrower than in the upper section. Values range mostly between 0.001 to 0.01 mm. Very few fractures have apertures greater than 0.01 mm reaching at most 0.04 mm. No relationship was observed between fracture aperture and the fracture orientation in the lower section.

Fracture density along the upper section never reach 8 fractures per meter (Figure 2), while in the lower section it can reach up to 12 fractures per meter in certain depths. Most of the above mentioned intervals are related to high gas shows from mud logging.

Average porosity observed was 0.7 to 0.8% for the entire logged interval. Some intervals reach up to 2% of fracture porosity. The main reason for this is the concentration of high fracture density (up to 12 fractures per meter) together with the high fracture apertures (up to 0.04 mm). One reason for the high apertures can be the shaly characteristic of this interval, which because of the relatively low Rxo value, probably increased the apertures, and then increase the fracture porosity. The steep fracture dips observed in these zones (65^o to 90^o) would also give high apertures when compared to other open fracture sets. Porosity was estimate without taking into consideration the fracture dips. Normally, we can expect that the steep fractures would give higher porosities due to their naturally higher apertures.

CONCLUSIONS

This work has shown how powerful the integration of downhole electrical images and the dipole sonic data can be for fracture interpretation. The orientation of the different sets of open fractures and the identification of the main fractured zones are important parameters in the development of this fractured reservoirs. The average aperture values computed from the electrical images range from 0.01 to 0.04 mm. Higher values appear within intervals with high dip magnitudes.
In the computation of fracture porosity, this work shows that care should be taken regarding the scale where the porosity computation is being performed. Anomalous porosity values were observed where high dip magnitudes are present. Differences in dips between sets of fractures can lead to different fracture porosity due to differences in fracture aperture.
The use of DSI data, both the VDL and the STC presentations together with the WAVENE processing, are very helpful in identifying open fracture zones. The correlation between the different techniques is very clear in the example above.

REFERENCES

Aguillera, R., 1995, Naturally Fractured Reservoirs. Penwell books. Tulsa, Oklahoma, 2nd edition, 520 p.

Luthi, S.M. and Souhaite, P., 1990, Fracture apertures from electrical borehole scans. Geophysics, 55, 7, 821-833.

Nelson, R.A., 1985, Geologic analysis of naturally fractured reservoirs. Cont. in Pet. Geology and Eng. Gulf Pub. Co.

Schlumberger, 1989, *Log Interpretation principles and Applications*. Schlumberger Educational Services, Houston TX.

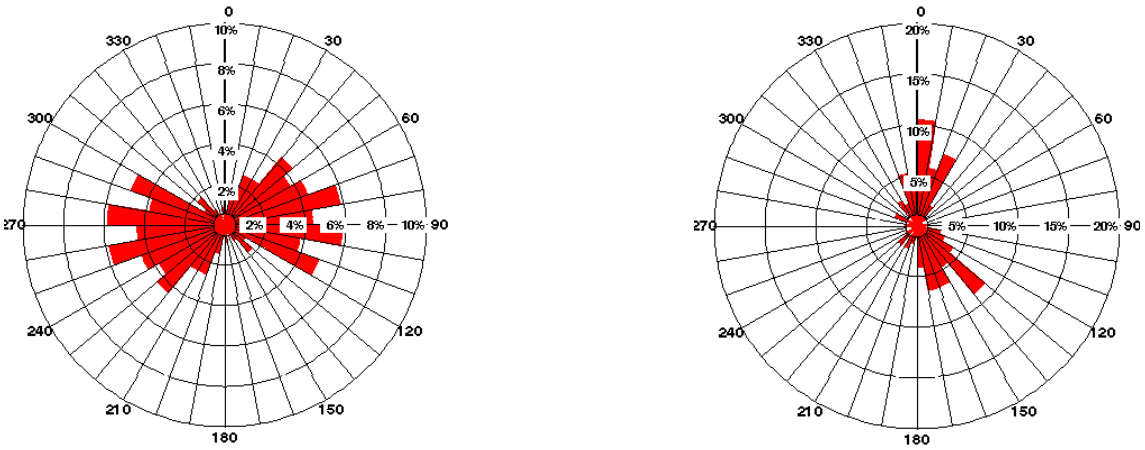

Figure 1 – Rosette Strike and Rosette Azimuth for open hole fractures in well XX (FMS logged section).

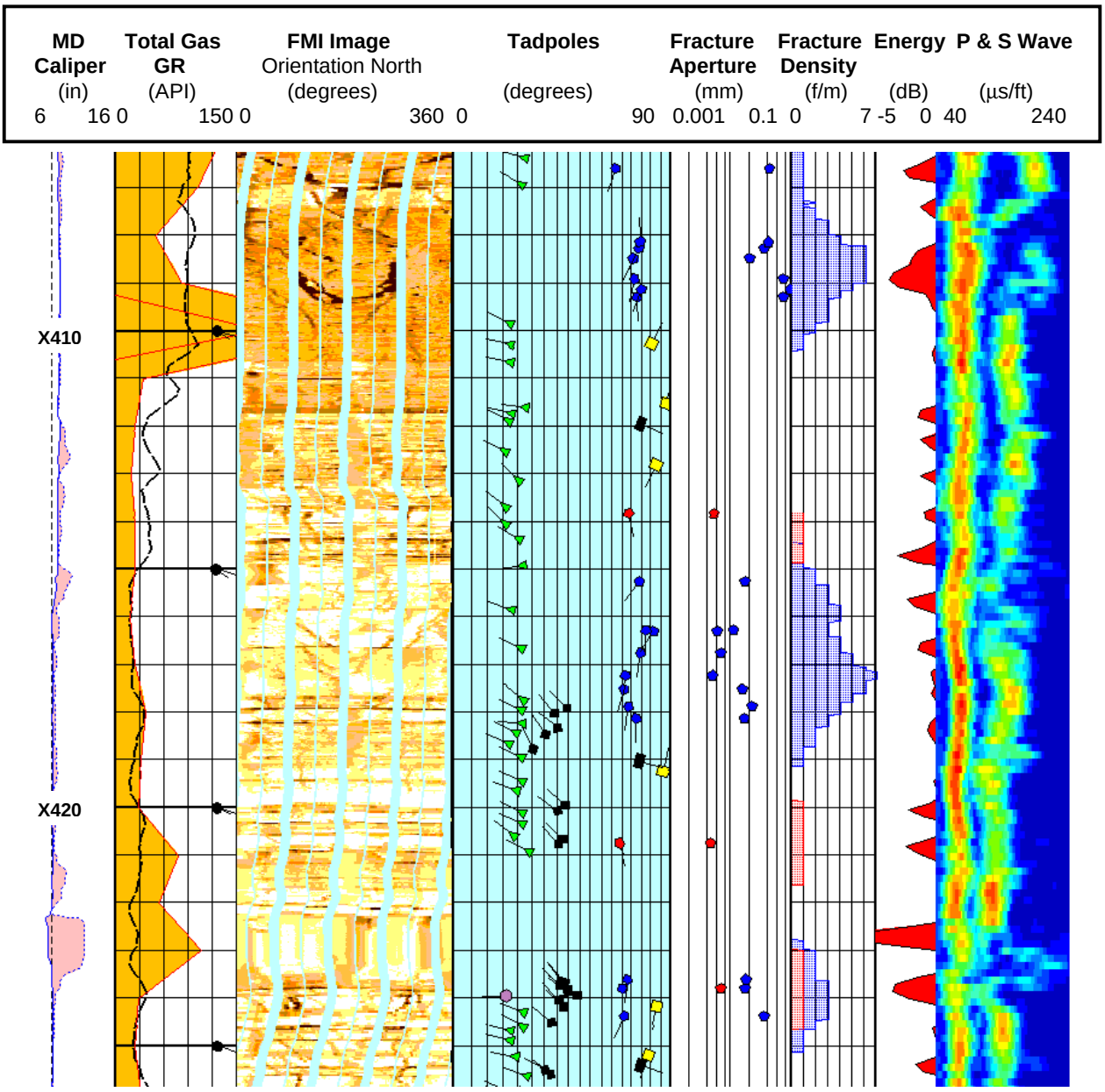

Figure 2 – Interval between X406 and X426 meters showing a FMI interpretation over a fractured zones. Track 1 shows measured depths and both caliper curves indicating hole ovalization. Track 2 shows gamma-ray curve and total gas from mud logging. Total Gas curve may not be depth matched with wireline logs.Track 3 shows the FMI static image. Note the change in the images between the silty shale above and the sandstone below. Track 4 shows the tadpoles from the FMI interpretation, where structural bedding are represented in green, cross-bedding in black diamond, open fractures are represented in blue and red for both sets mapped in the upper section of the well, black squares represent breakouts while yellow squares represent induced fractures. Track 5 shows the apertures (ranging from 0.001 to 0.1 mm) for the open fractures. Track 6 shows fracture density per meter ranging from 0 to 7 fractures per meter. Track 7 contains the stoneley wave energy attenuation. Higher attenuations are related to the presence of fractures. Last, track 8 shows the STC processing for the P&S mode of the DSI tool, where shear wave transit time are disturbed in high fracture density zones.